# Wakes in very large wind farms and the effect of neighbouring wind farms

**Nicolai Gayle Nygaard**

DONG Energy Wind Power
Kraftværksvej 53, 7000 Fredericia, Denmark

nicny@dongenergy.dk

**Abstract**. We present the first analysis of wake losses in some of the largest offshore wind farms built to date. In addition, we give an example of the external wake losses that can be imposed by a neighbouring wind farm. Both situations lend insights to the wake phenomena in large offshore wind farm clusters. A simple wake model is compared to the data to assess the need for a more detailed physical description of large wind farm wakes.

## 1. Introduction

The next generation of offshore wind farms have capacities of several hundred MW. In addition, offshore wind farms are now constructed in clusters, where neighbouring wind farms impact each other. This is a new regime for the wind energy industry, which may require a new modelling paradigm. Turbines in a large array are known to alter the flow in the atmosphere above the wind farm [1,2]. It has been proposed that this hampers the entrainment of momentum from the air above the wind farm, restricting the wake recovery. This is called the deep array effect. Preliminary evidence of the deep array effect has been presented for the offshore wind farms Horns Rev 1 and Nysted [3–7] as well as for onshore wind farms [5,8]. This has prompted the development of extensions to engineering wake models to remedy the perceived underestimation of the wake losses inside large arrays. However, the fundamental question remains, is the deep array effect real? Can the current generation of wake models without explicit corrections for large wind farms accurately account for wake effects on the regional scale of a very large wind farm or a wind farm cluster? As data from offshore wind farms with capacities exceeding 350 MW are becoming available, we can begin to address these issues systematically.

In the first part of the work presented here we investigate power and wind speed ratios along rows of turbines in three very large offshore wind farms: Walney (102 turbines), Anholt (111 turbines), and London Array, which with its 175 turbines is currently the largest offshore wind farm in the world. This allows us to highlight any possible change in the nature of wake recovery deep inside a large wind farm. Furthermore, the Walney Offshore Wind Farm is divided evenly into two sub-farms that have turbines with different hub heights and rotor diameters and were constructed almost a year apart. Hence we can observe the role of rotor size in the wake losses. Additionally, by comparing results before and after the completion of the second phase of construction, we can address the effect of doubling the size of the wind farm. We compare our observations with a simple engineering wake model to assess the model performance for very large arrays and for layouts with mixed turbine types.

In the second part of the study we compare the wake losses at Nysted before and after the construction of the nearby wind farm Rødsand II. We quantify the increase in the wake losses for particular wind directions, and also observe the effect of Rødsand II on the turbulence experienced by the Nysted turbines. In the following section we give a brief account of the wind farms included in this study and of the methods used in the data analysis. The wake modelling is outlined in Section 3. Sections 4 and 5 present the results for wake losses in very large arrays and the effect of neighbouring wind farms, respectively. The final section summarises the conclusions reached.

## 2. Data

The wind farms included in this study are listed in Table 1. Walney (Walney 1 and Walney 2), London Array and Anholt are some of the largest offshore wind farms in the world and were all commissioned in or after 2010, while Nysted is an older wind farm commissioned in 2004. Nysted is included here to assess the impact of the neighbouring wind farm Rødsand II, which has 90 turbines with a rated capacity of 2.3 MW, hub height of 68.5 m, and a rotor diameter of 93 m. The locations of the wind farms are indicated in Figure 1.

**Table 1.** Characteristics of the wind farms included in the analysis.

| **Wind farm** | Walney 1 | Walney 2 | London Array | Anholt | Nysted |
|---|---|---|---|---|---|
| **Capacity [MW]** | 183.6 | 183.6 | 630 | 400 | 165.6 |
| **Number of turbines** | 51 | 51 | 175 | 111 | 72 |
| **Hub height [m]** | 83.5 | 90 | 84.5 | 82 | 68 |
| **Rotor diameter [m]** | 107 | 120 | 120 | 120 | 82 |

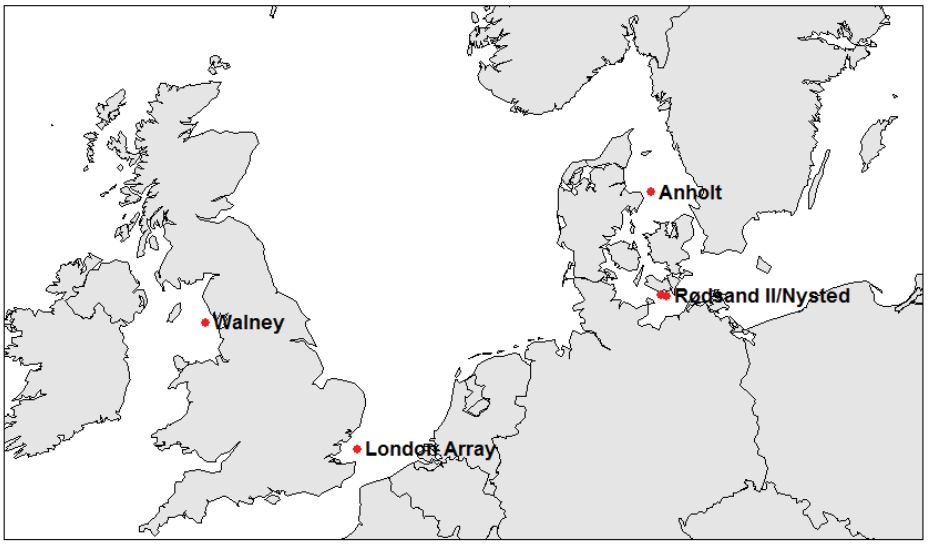


**Figure 1.** Map of the wind farms featured in this study.

For each wind farm 10-minute averaged data from the Supervisory Control And Data Access (SCADA) system was downloaded and the following steps were undertaken. First, the wind direction was derived from a farm average of the turbine yaw directions. This constructed direction generally contains an offset, which we remove by calibrating the wind direction against the expected direction of maximum power deficit between two turbines in the first and the second row of the wind farm [9]. Since the offset can be time-dependent, the calibration is performed in a moving time window. Next we derive the wind speed from the turbine power production and the manufacturer's power curve. The

free wind speed can then be estimated by averaging the wind speed of the upstream turbines exposed to undisturbed inflow. Finally, the data for each turbine is filtered according to the criteria that the turbine is available to produce power throughout the 10-minute period, and that it is not curtailed. When analysing wake losses along a wind farm transect, all turbines in the row and 95% of all turbines in the array are required to be operational.

## 3. Wake model

We base our analysis on arguably the simplest model for wind turbine wakes. The Jensen model [10] was proposed more than 30 years ago in an era of much smaller turbines and wind farms, yet it continues to be a workhorse in the wind energy industry and it is a standard tool in commercial software packages such as WAsP [11]. Our implementation of the Jensen model differs from that in WAsP in one aspect: we do not include "image turbines" to account for a reflection of the wake as it impact the surface. The combination of multiple, overlapping wakes is through a quadratic superposition [12]. We refer to the original publications for the mathematical details. It suffices to state here that the model contains a single parameter, the wake decay parameter, which specifies the rate of the linear expansion of the wake with downwind distance. Based on previous benchmarking results for offshore wind farms we use a value of 0.04 for the wake decay parameter.

## 4. Wake losses in very large arrays

This section focuses on the power loss along transects of turbines in very large wind farms. Specifically, our aim is to address whether the Jensen wake model can continue to accurately account for wake losses as the typical size of an offshore wind farm is increased. Wind resources assessment usually subdivides the wind direction into 12 evenly spaced sectors of 30°. To stay true to this practise and to avoid issues with the wind direction uncertainty for smaller sectors [13] we investigate the ability of the wake model to predict the power ratio of turbines in the transect, when the observational data is averaged in a sector of this size. The modelled wake losses are calculated at 1° increments in the studied sector, and the results are averaged and compared with the observations. In all subsequent plots error bars or shaded error bands on the experimental results represent the 95% confidence interval of the mean value. Unless stated otherwise transect power ratios are relative to the first turbine in the row.

The Walney offshore wind farm consists of two sub-farms, Walney 1 and Walney 2, commissioned 10 months apart. In Figure 2, we illustrate the impact of Walney 2 on the wake losses in Walney 1, by comparing the power loss along a line of turbines in Walney 1 (red filled circles in the wind farm layout in Figure 2a) before and after the construction of the Walney 2 sub-farm. In the latter case the wind passes through Walney 2 before reaching Walney 1. We normalise with the power production at the *second* Walney 1 turbine in the row (B09), to make the relative production of the Walney 1 turbines before and after Walney 2 comparable. The effect of the second sub-farm is to make the power ratios along the transect more alike, indicating a balance between power losses in consecutive, overlapping wakes and replenishment of momentum from the outside, primarily from above. In Figure 2c we plot the turbulence intensity based on the nacelle anemometers of the turbines in the transect. This is not an accurate measurement, due to the flow disturbances presented by the rotor and the nacelle, but we take it to be representative of the general trends of the turbulent inflow and hence useful for the comparative analysis. This shows an increased turbulence level in the wake of Walney 2, which facilitates a faster wake recovery. Towards the end of the Walney 1 transect Walney 2 has a diminishing impact on the turbulence intensity.

In Figure 3a the turbine power production (relative to the front turbine) is plotted along the same transect, but now including the turbines in Walney 2. The production values are normalised to the frontline turbine B18. The rotor diameter of the Walney 2 turbines is 12% larger than for Walney 1. The power production therefore drops between the eighth and the ninth turbine in the row. Otherwise

it is very flat along the transect 2-3 turbines after the gap in the layout. Plotting the ratios of the wind speeds derived from the SCADA data as in Figure 3b the difference between the Walney 1 and Walney 2 turbines is less pronounced, underlining the more or less constant nature of the wake loss for the majority of the 18 turbines in the transect. The black lines in Figure 2b and Figure 3 represent the result of the Jensen wake model before and after Walney 2, respectively. In both cases the model predictions fit the observations well with no significant underestimation of the wake losses and hence no evidence of a deep array effect.

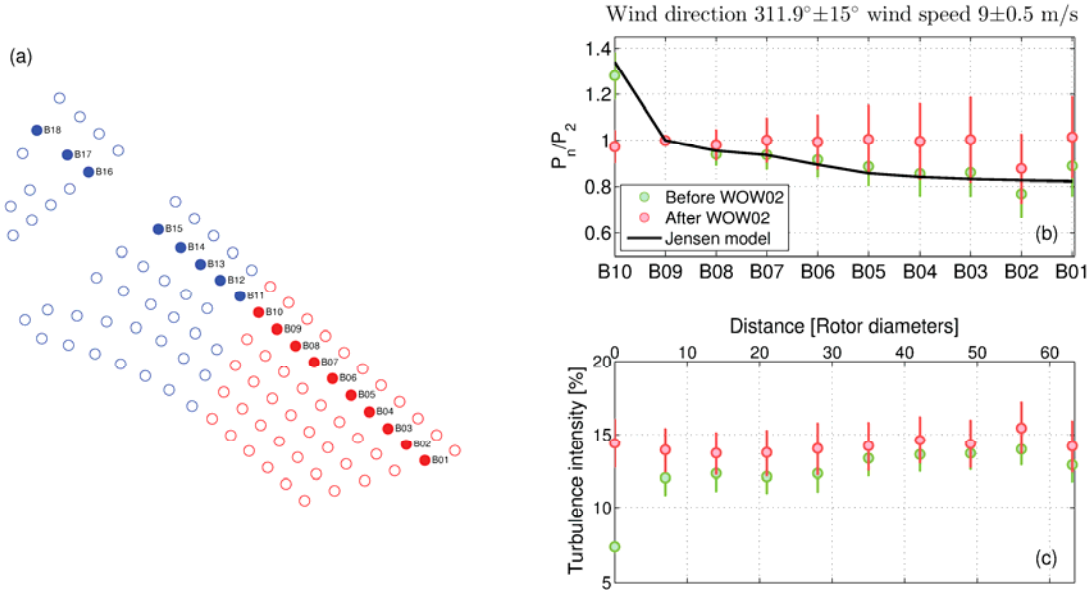


**Figure 2.** (a) Walney 1 (red) and Walney 2 (blue) wind farms. The filled circles mark the analysed transect. (b) The power ratio for turbines along the transect, normalised to B09, the second Walney 1 turbine in the transect. (c) The turbulence intensity based on the nacelle anemometer of the Walney 1 turbines along the transect. In (b) and (c) green (red) circles represent data collected before (after) commissioning of Walney 2. The modelled wake loss before Walney 2 is the black line in (b).

Next, we turn our attention to London Array, where we present power ratio results for four different transects. Two in a north-western wind direction sector with a turbine spacing of 5.4 rotor diameters, and two aligned with south-western winds where the turbines are 8.3 rotor diameters from one another, see Figure 4a. In both sectors we analyse an interior row/column in the mostly regular matrix layout as well as a more exterior row/column. If the deep array effect does occur, the interior turbines far downstream should have higher wake losses than the turbines closer to the edge of the array, since the latter are exposed to fewer overlapping wakes. For the north-west sector centred on 312.2° the wake losses in the two transects are practically identical, and both are well-described by the Jensen model. As in the case of Walney the power ratio stabilises after a number of turbines. In contrast, for the south-western sector the interior and the exterior transects are quite different. In particular, while the results for the C19-M19 turbines are also in broad agreement with the wake model, the model underestimates the wake losses along the A13-L13 transect, as the observed power continues to drop through the array. This is similar to what the observations at Horns Rev 1 and Nysted, which led to the postulation of the deep array effect [3–6].

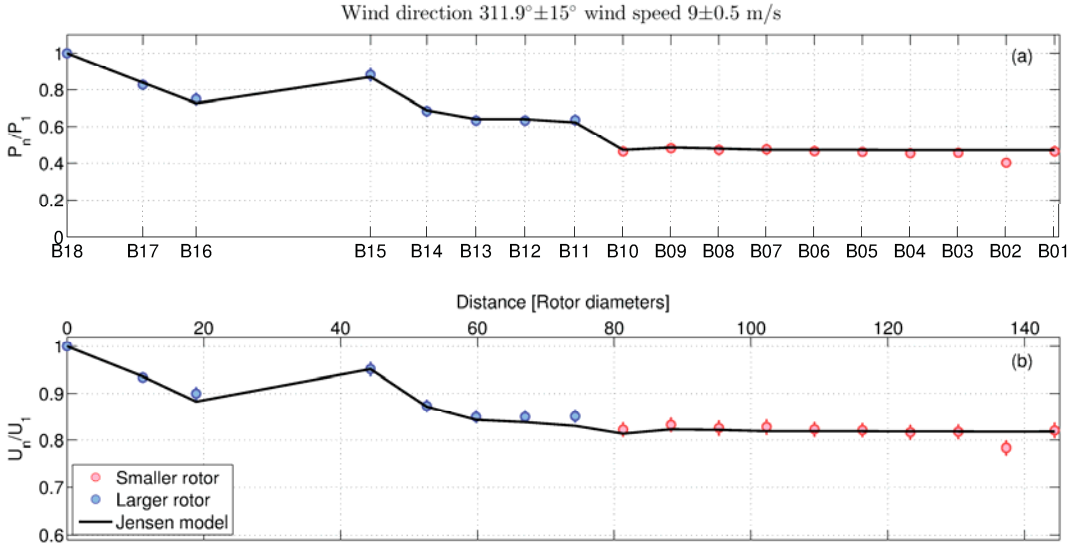


**Figure 3**. Power ratio (a) and wind speed ratio (b) along the same Walney transect as in Figure 2. Blue circles are Walney 2 turbines, while turbines in Walney 1 are marked with red circles. The black lines are the Jensen model results. Distance is measured in Walney 1 rotor diameters.

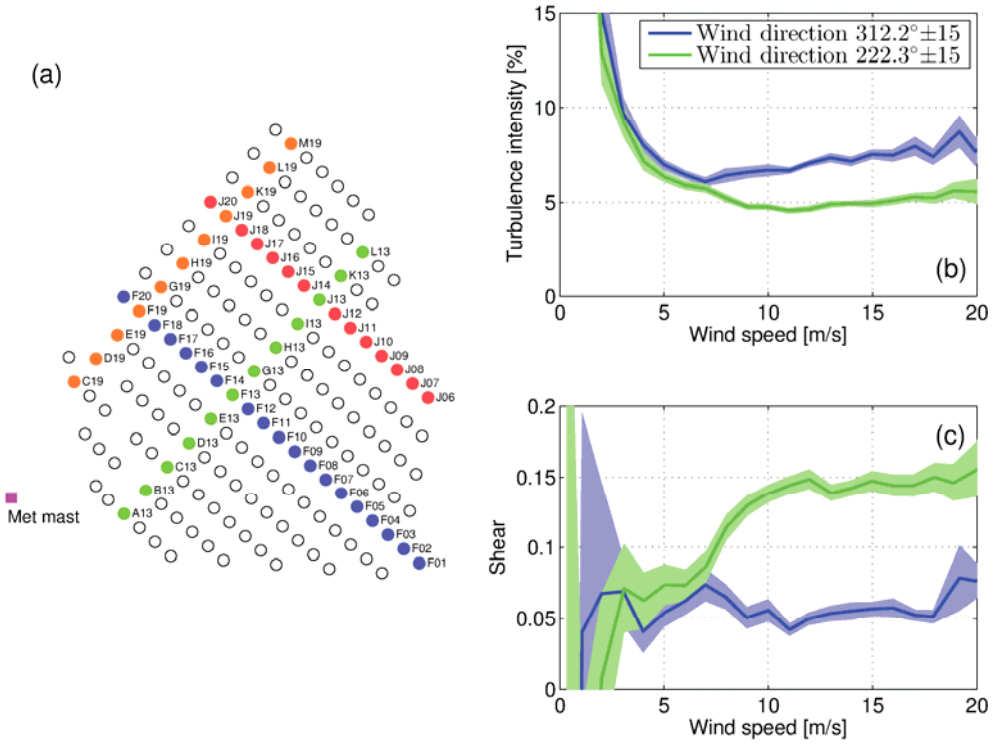


**Figure 4.** (a) Layout of London Array. The filled circles denote the selected transects. The square is the met mat (b) Turbulence intensity as a function of wind speed as measured by the met mast top anemometer. (c) Shear determined from a power law fitted to wind speeds at two heights at the mast.

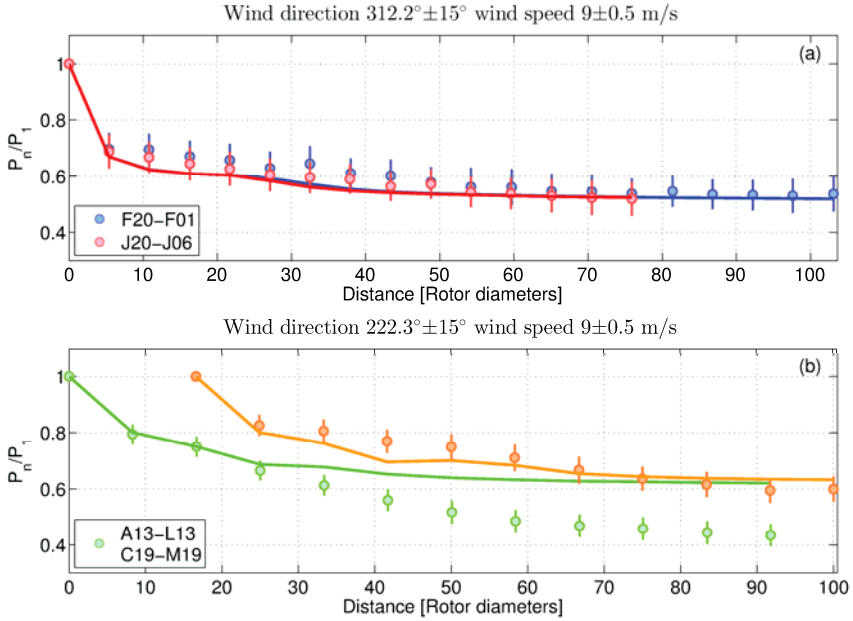


**Figure 5.** London array transect plots. (a) Power ratios along transects in the north-west sector. (b) Power ratios along transects in the southwest sector. The transects are identified in the layout in Figure 4. The solid lines represent the power values predicted by the Jensen wake model.

We believe that the differences between the two sectors are not related to the structure of the array, but that the cause is to be found in a difference in inflow conditions. This is suggested by comparing the turbulence intensity and shear measured in the two sectors at the met mast situated to the west of the wind farm. These are shown as a function of wind speed in Figure 4b and c, respectively, and cover the same time period as the SCADA data. At 9 m/s the turbulence intensity in the south-western sector is significantly lower than in the north-west sector. At the same time the wind shear is considerably higher for the sector centred around 222.3°. For both sectors the mast is in free flow, so it is not clear why the conditions in the two sectors are so different. The plots reveal that the inflow conditions are similar at lower wind speeds. To test the impact of this on the wake losses we plot in Figure 6 the same transect power ratios at 6 m/s. At this wind speed the wake model captures the asymptotic behaviour in all four transects, and notably the difference between the power ratios far downstream in the two transects in the south-western sector has disappeared. Hence we find no robust evidence of the deep array effect. More work is needed to resolve the differences we observe, but it is known that a smaller turbulence intensity leads to enhanced wake losses [14]. Peña *et al* have proposed a modification of the Jensen model where the wake decay parameter is proportional to the ambient turbulence intensity [15]. Figure 10 of Peña *et al* demonstrates that a smaller wake decay parameter can account for the continued increase of the wake loss in Horns Rev 1. Less turbulence leads to less mixing and hence narrower wakes, which recover slower. This in turn gives rise to larger losses, consistent with the results for London Array at 9 m/s, though this does not account for the difference between the two south-western transects.

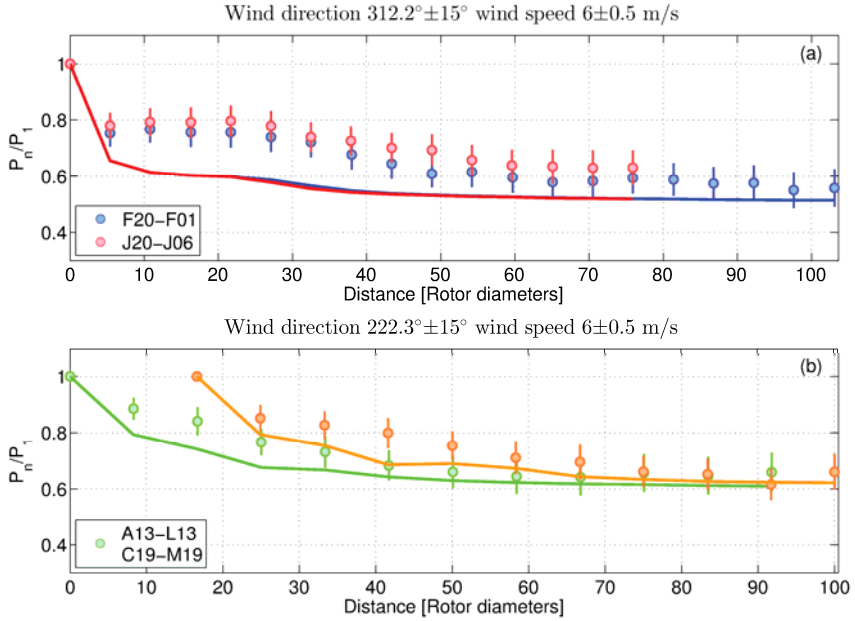


**Figure 6.** Same transects as in Figure 5 but for wind a wind speed bin where the two sectors experience the same ambient turbulence intensity.

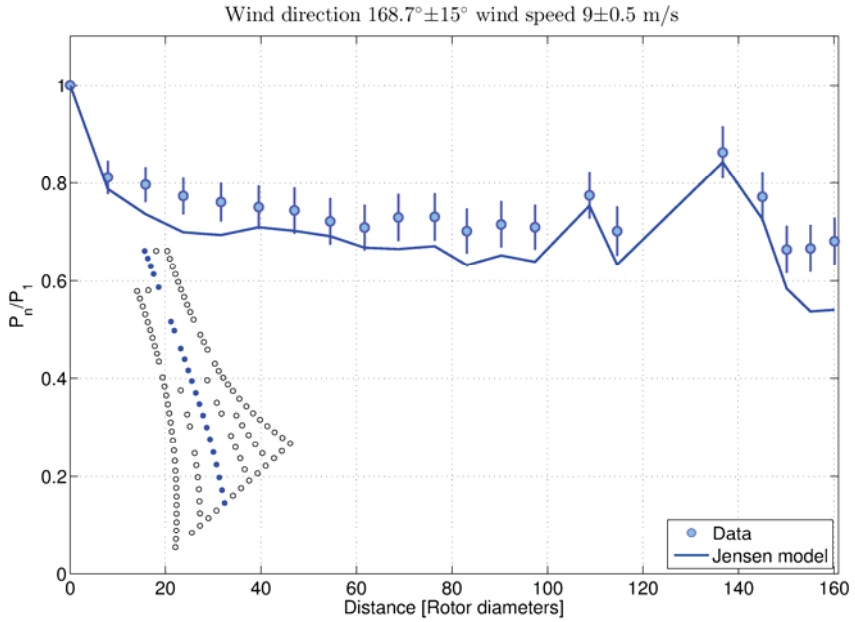


**Figure 7.** Power ratio along a transect in Anholt. The transect is marked by the filled circles in the layout in the inset. The solid line is the wake model result.

The last offshore site we consider for possible large wind farm effects is Anholt. In contrast with both Walney and London Array, and indeed most other offshore wind farms, Anholt has an irregular layout (see inset in Figure 7). The large concentration of turbines on the perimeter leaves the wind farm interior open and minimises the wake losses, which are about half of those experienced at

Walney with roughly the same number of turbines. In Figure 7 we plot the power ratio along the central transect for wind directions in a southern sector. Consistent with the preceding results the wake model shows no underestimation of the wake losses, and the power ratio reaches a steady-state of little further loss near the middle of the transect. There is slightly more variation from turbine to turbine than seen in the other wind farms in this study, due to a gap after turbine 16, an uneven spacing between the turbines in general and a slight curvature of the row.

## 5. Effect of neighbouring wind farms

In this section we demonstrate the impact of the Rødsand II wind farm on the energy production at Nysted. The two wind farms are separated by 3 km with Rødsand II placed upstream of Nysted in the predominant wind direction. Since Rødsand II is operated by another developer, we do not have access to SCADA data from the upstream turbines. However, Nysted was constructed some years before Rødsand II, so we have the opportunity to perform a pre-/post-Rødsand II comparison on Nysted alone. We use turbine A01 in the north-western corner of the wind farm as a reference (this turbine is marked with a square in Figure 8). This is not ideal as it is strictly speaking in the wake of turbines in the north-western corner of Rødsand II after their commissioning. However, the wake effect from these turbines is diminished by the large separation. In addition, the inflow at turbine A01 may be subject to disturbances and blockage by Rødsand II, which makes it distinct from the free inflow. Nonetheless this is the best reference turbine we can choose, but the caveats just mentioned must be kept in mind when interpreting the results.

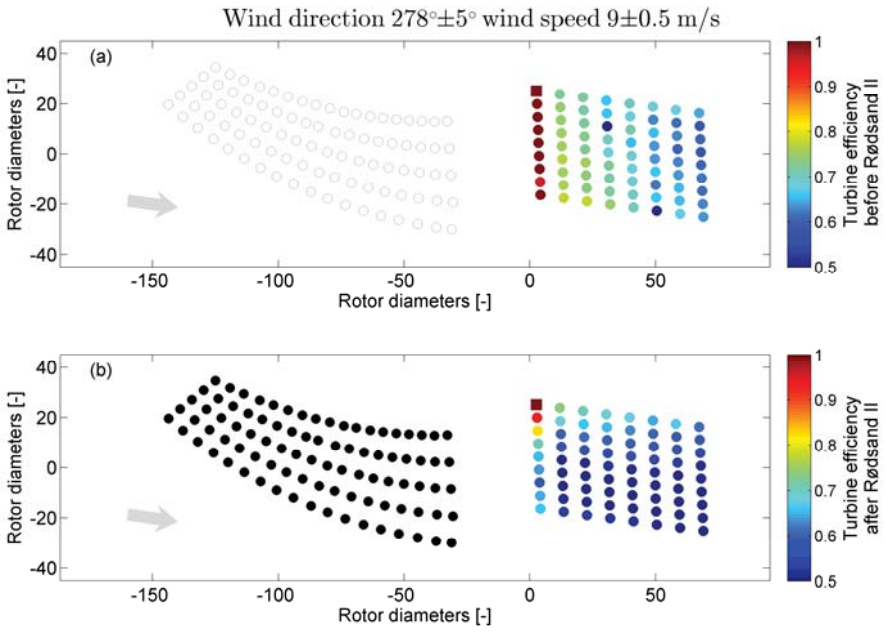


**Figure 8.** Layout of Rødsand II (left) and Nysted (right). The colour indicates the efficiency for the individual Nysted turbines. The wind direction is shown with the grey arrow, while the reference turbine is marked with a square. (a) Before Rødsand II. (b) After Rødsand II.

The effect of Rødsand II on the individual turbines in Nysted can be gauged visually in Figure 8 by comparing panels (a) and (b), which show the turbine efficiencies before and after commissioning of Rødsand II, respectively. The turbine efficiency is defined here as the ratio of the average turbine power and the mean production of the reference turbine. Only data corresponding to the chosen flow case (wind direction in a sector aligned with the west-east rows of Nysted and reference wind speed in

the range 8.5-9.5 m/s) and with more than 95% of the Nysted turbines fully operational have been included in the averaging. Before Rødsand II the pattern of turbine efficiencies conform well to the geometry of the wind farm, with a couple of outliers producing below the level of comparable neighbours. The reason for these outliers was not investigated as it does not impact the conclusions presented here. Once Rødsand II is operational the efficiency of the Nysted turbines is reduced especially in the southern half of the wind farm. The drop in efficiency is generally larger for turbines further upstream.

As the annual energy production is the key financial driver for a wind farm project it is relevant to ask how the upstream wind farm impacts the amount of energy produced by the downstream neighbour. To answer this question we find the wind farm efficiency as a function of wind direction. This is defined in much the same way as the turbine efficiency above, but the averaged quantities are the total wind farm production and the gross power of the entire wind farm. To increase the data volume we allow as before up to 5% of the turbines to be not producing or curtailed. The total wind farm power and gross power values are adjusted to the instantaneous number of turbines with valid data. The result in Figure 9a shows that the wind farm efficiencies before and after Rødsand II are almost identical for all wind direction except for the sector between about 240° and 300°. In this sector the efficiency is reduced due to the wake losses from Rødsand II. The lower panel in the figure shows the variation of the turbulence intensity from the nacelle anemometer of turbine A06. There is a large variation with peaks corresponding to internal wakes from other Nysted turbines, but it is also clear that the turbulence intensity is elevated in the sector where Nysted is in the wake of Rødsand II due to wake-added turbulence from the neighbouring wind farm.

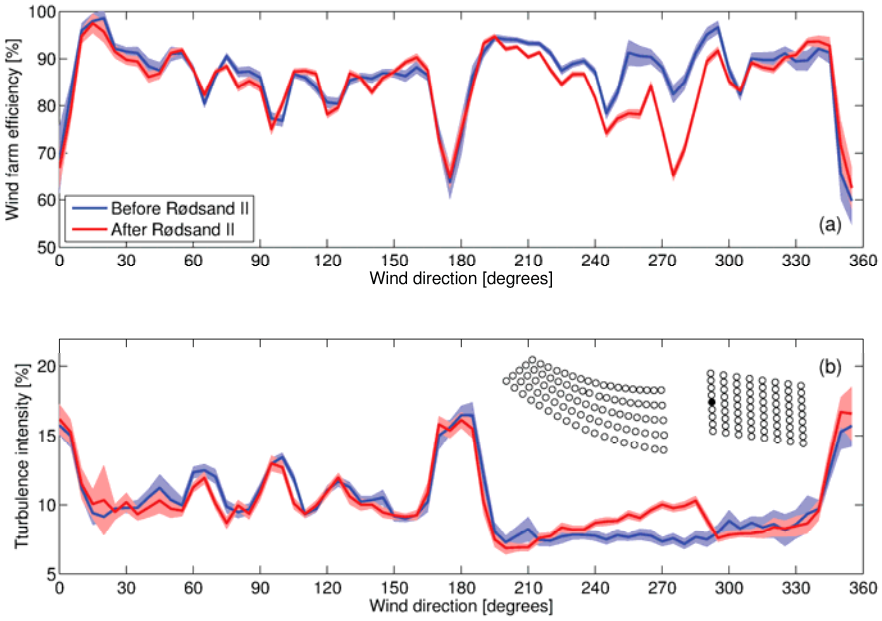


**Figure 9.** (a) Wind farm efficiency for Nysted. (b) Nacelle anemometer turbulence intensity at turbine A06 (filled circle in the inset). Blue (red) curves apply before (after) construction of Rødsand II.

## 6. Conclusions

We have presented the first analysis of wake losses in three recently completed offshore wind farms. Our analysis shows that no new regime is realised when the size of an offshore wind farm exceeds 100 turbines. The notable exception is the interior transect in the south-western sector for London Array,

where the model underestimates the wake losses dramatically. However, since the agreement between model and observations is improved by choosing a different flow case corresponding to a higher ambient turbulence intensity, we speculate that the disagreement is not a result of the wind farm size, but of the wake model overestimating the wake width in low turbulence conditions. If this is confirmed it indicates that the wake model can be improved by including turbulence explicitly (or implicitly through a stability parameter) through the value of the wake decay parameter.

In addition, we have quantified the impact of a neighbouring wind farm on the energy production and the turbulence intensity. We find that the external wake losses can be significant for wind directions, where the neighbouring wind farm is directly upstream. This additional wake loss is accompanied by an increase in the turbulence intensity on the order of a few percent.

In future work we will compare the observed wind farm efficiency with that predicted by the wake model to assess the overall accuracy of the Jensen model when estimating the annual energy production of large offshore wind farms. Furthermore, a turbulence specific version of the wake model (like the extended PARK model [15]) should be tested against the data. Likewise, the observations should be reconciled with fluid dynamic models, providing a deeper physical understanding through simulation of the interaction of the wind farm with the planetary boundary layer.

**References**

[1] Calaf M, Meneveau C and Meyers J 2010 Large eddy simulation study of fully developed wind-turbine array boundary layers *Phys. Fluids* **22** 015110
[2] Chamorro L P and Porté-Agel F 2011 Turbulent Flow Inside and Above a Wind Farm: A Wind-Tunnel Study *Energies* **4** 1916–36
[3] Schlez W and Neubert A New Developments in Large Wind Farm Modelling *EWEC 2009*
[4] Barthelmie R J and Jensen L E 2010 Evaluation of wind farm efficiency and wind turbine wakes at the Nysted offshore wind farm *Wind Energy* **13** 573–86
[5] AWS Truepower 2011 *The openWIND Deep-Array Wake Model Development and Validation*
[6] GL Garrad Hassan 2012 *WindFarmer V5.0 Validation Report*
[7] Smith G M, Neubert A and Schlez W Impact of Large Neighbouring Wind Farms on Energy Yield of Offshore Wind Farms *EWEA Offshore 2011*
[8] Louro A On-Shore Wake Validation Study *Brazil Windpower 2013*
[9] Réthoré P-E, Johansen N A, Frandsen S T, Barthelmie R, Hansen K S, Jensen L E and Bækgaard, Mikkel A.B. Kristoffersen J R 2009 Systematic wind farm measurement data reinforcement tool for wake model calibration *EOW Conference*
[10] Jensen N O 1983 *A Note on Wind Generator Interaction, Risø-M-2411*
[11] www.wasp.dk
[12] Kátic I, Højstrup J and Jensen N O 1986 A simple model for cluster efficiency *EWEA 1986*
[13] Gaumond M, Réthoré P-E, Ott S, Peña A, Bechmann A and Hansen K S 2013 Evaluation of the wind direction uncertainty and its impact on wake modeling at the Horns Rev offshore *Wind Energy* doi: 10.1002/we.1625
[14] Hansen K S, Barthelmie R J, Jensen L E and Sommer A 2012 The impact of turbulence intensity and atmospheric stability on power deficits due to wind turbine wakes at Horns Rev wind farm *Wind Energy* **15** 183–96
[15] Peña A, Réthoré P-E, Hasager C B and Hansen K S 2013 Results of wake simulations at the Horns Rev I and Lillgrund wind farms using the modified Park model *DTU Wind Energy-E-Report-0026(EN)*
[16] Cleve J, Greiner M, Enevoldsen P, Birkemose B and Jensen L 2009 Model-based Analysis of Wake-flow Data in the Nysted Offshore Wind Farm *Wind Energy* **12** 125–35